Expanding Underground. Knowledge and Passion to Make a Positive Impact on the World – Anagnostou, Benardos & Marinos (Eds)

Equivalent material modelling of fractured rock mass resonance effects

H.T. Holmes, C. Paraskevopoulou & M. Hildyard
University of Leeds, Leeds, UK

K. Neaupane
AECOM UK&I, Birmingham, UK

D.P. Connolly
University of Leeds, Leeds, UK

ABSTRACT: Resonance effects in parallel fractured rock masses are investigated using equivalent material models. The mechanisms of spring resonance and superposition resonance are considered. Both of these resonance mechanisms give rise to resonant frequencies, which represent bands of high transmission. Three different representations of a fractured rock mass are adopted: discrete fractures using special elements in the finite difference mesh; a homogenous equivalent medium representing the weakening to the material caused by the fractures; and a localised equivalent medium applied in the vicinity of fractures. The models are excited by a wide-band source, the response measured and a transfer function generated from the results. Results are compared to the prediction of spring and superposition resonant frequencies calculated using analytical equations. It is found that the discrete and localised equivalent materials give similar results, which match the predictions from the analytical equations for both resonance mechanisms, while the equivalent homogenous medium does not show any resonance effects. Showing that this effect occurs in the appropriate equivalent material model helps future prediction of ground borne vibrations from underground sources, such as railway tunnels, as it gives a greater scope of models which can accurately model the propagation of stress waves through fractured rock masses.

1 INTRODUCTION

Fractured rock masses are common in nature and have been the subject of numerous studies in the past. Vibrations propagating through fractured rock masses are a subject area with a rich history. The motivation of this work is to study vibrations propagating through fractured rock masses generated from trains running through tunnels (Figure 1). Trains in tunnels generate ground borne vibrations at a range of frequencies, typically up to 250Hz (Ouakka et al., 2022). Understanding the propagation of vibrations from train tunnels to receptors is a well researched subject (Avci et al., 2020; Forrest and Hunt, 2006; M. F. M. Hussein et al., 2014; Ruiz et al., 2019; Sheng, 2019). However, studies of the transmission of stress waves through fractured rock masses and studies from stress waves generated by rail vibrations tend not to overlap, with few exceptions (Eitzenberger, 2012). Therefore, a gap does exist in the available literature for studying rail vibrations, generated within tunnels, propagating through fractured rock masses.

DOI: 10.1201/9781003348030-33

Stress waves propagating through a fractured material are affected by differences in the seismic velocity of blocks and the presence of discontinuities. Propagation of stress waves can be refracted and reflected at interfaces between blocks. When two blocks are in contact and their seismic velocity is the same, refraction and reflection occurs if the two blocks are not perfectly bonded, giving a finite fracture stiffness. If the blocks are perfectly bonded the interface is effectively not there and no refraction or reflection occurs. In reality, fractures will not be perfectly bonded and will have a finite fracture stiffness due to roughness of the fracture walls, infilling of the fracture or a weathered annulus in the blocks on either side of the fracture (Bandis et al., 1983). This will be the case in a homogenous fractured rock mass, where the rock mass is composed of blocks of the same properties separated by fractures. Stress wave propagation through fractures has been widely studied in literature with analytical solutions being derived for a variety of situations (Cai and Zhao, 2000; Pyrak-Nolte et al., 1990), as well as more complex cases being investigated numerically (Deng et al., 2012; Fan et al., 2018; Hildyard, 2007; Holmes et al., 2022; Parastatidis, 2019; Xu et al., 2022). For single fractures, the degree of reflection is related to the fracture stiffness and the frequency of the incident wave. The degree of reflection increases as the stiffness of the fracture reduces; with a very low stiffness fracture reflecting all energy and a very high stiffness fracture transmitting all energy. Incident waves of a high frequency will also show a greater degree of reflection than low frequency waves. Cai and Zhao (2000) found that when there are multiple parallel fractures a relatively high transmission zone can develop at low frequencies. This only occurs at very specific ratios of fracture spacing to wavelength, but indicates that there are many factors to consider between fractured rock masses and wave transmission.

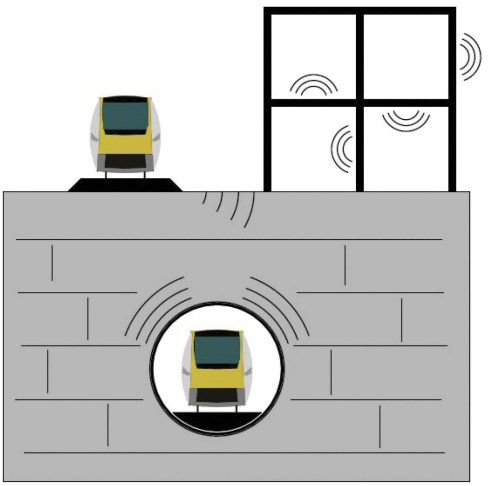

Figure 1. Train vibrations from embankments and tunnels in jointed rock masses.

Holmes et al. (2022) investigated resonance effects within parallel fractured rock masses, finding that there are two mechanisms which allow high transmission. These are superposition resonance and spring resonance. Superposition resonance is generated through the constructive interference of reflected waves, causing standing waves to develop within blocks. Spring resonance occurs when fracture bounded blocks oscillate like masses between springs. Equations to predict the frequencies of these resonance effects were presented, which are included in equations 1 and 2, for spring resonance, and equation 3, for superposition resonance. The superposition resonance effect has been identified previously by Li et al. (2019) and Nakagawa (1998). Due to the high velocity of intact rock material, superposition resonance typically occurs at high frequencies, often outside the range of train vibrations. The spring resonance effect has not previously been identified in fractured rock masses, despite its foundation in classical mechanics. However, it has been described in 1D monatomic phononic crystals

(Hussein et al., 2014). These tend to occur at lower frequencies, which can potentially affect the frequency of vibrations from railways. Knowing the resonant frequencies of a fractured rock mass, and as a consequence the frequencies which will be preferentially transmitted, it is possible to more accurately predict the frequency of vibrations incident upon a receiver and as such design mitigation measures to reduce these vibrations.

$$K_m X = \alpha M X \tag{1}$$

$$f_n = \frac{1}{2\pi}\sqrt{\alpha_n} \tag{2}$$

$$f_n = \frac{nC_p}{2s} \tag{3}$$

Where, K_m is the stiffness matrix, M the mass matrix, X a vector which satisfies equation 1, α and α_n the eigenvalues and n'th eigenvalue of equation 1, C_p the p-wave velocity, n the resonant peak number and s the fracture spacing.

Holmes et al. (2022) generated models containing discrete fractures. However, the effect of different material models on these resonance mechanisms were not tested. Parastatidis (2019) analysed the effect of different fracture models on the propagation of stress waves. Discrete fractures, as used by Holmes et al. (2022), as well as equivalent transversely isotropic materials and localised equivalent materials were investigated. This study will model a fractured propagation pathway using the equivalent material models of Parastatidis (2019) in order to determine whether these resonance effects still persist.

2 METHODLOGY

A numerical model is used to evaluate the effect of different equivalent material models on resonance effects. The numerical model is solved using the finite difference method (FDM) in the software WAVE2D (Hildyard et al., 1995). The model used is a two-dimensional (2D) model with plane wave boundaries, which approximates a one-dimensional (1D) model. The model has boundaries of 384 m and 166.4 m, with a square finite difference mesh with 0.08 m edge lengths, chosen in order to allow transmission of high frequency waves given the

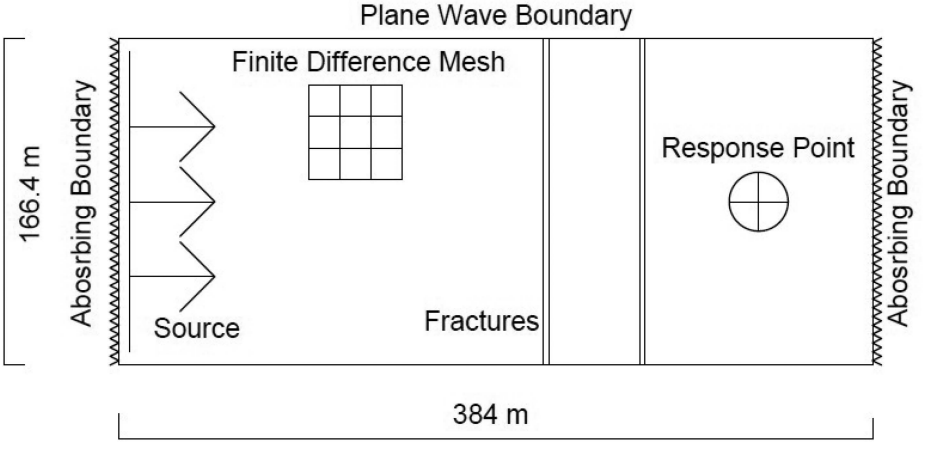

Figure 2. FDM Model showing finite difference mesh. Mesh fills entire model. Not to scale.

velocity of the materials (Table 1). A unit velocity source is applied to the left-hand boundary of the model, which propagates from left to right, with the response recorded close to the right hand boundary. The model is shown in Figure 2 with the source and its frequency content shown in Figures 3a and b, respectively. The wave shown in Figure 3 is used as it generates a wide frequency band.

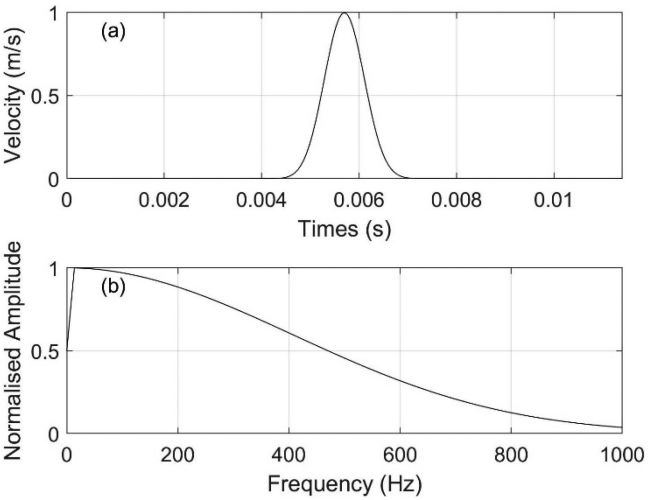

Figure 3. Source used in models. (a) velocity-time series, (b) frequency content.

Table 1 shows the material properties used throughout this study, which are those of a sandstone with a high strength. The selection of this material is arbitrary, although it was previously modelled by Holmes et al. (2022). No damping is applied in any of the models, in order to isolate the effect of the fractures on the transmission of stress waves.

Table 1. Model properties used for fractures and intact blocks.

Fracture Stiffness (kn)	1 GPa/m
Fracture Spacing (s)	2 m
Intact Material P-Wave Velocity (Cp)	3328 m/s
Intact Material S-Wave Velocity (Cs)	1922 m/s
Intact Material Density (ρ)	2600 kg/m^3

Fractures are shown in the model in Figure 2, although not all models in this study explicitly model fractures. Fractured materials can be modelled in a number of different ways, which tend to be split into the discrete representation of fractures and equivalent material methods. Parastatidis (2019) used three different methods, which can be split into these general areas, as shown by Figure 4. Using the FDM, fractures were represented as special elements in a discrete model, as described by Hildyard et al. (1995). Parastatidis (2019) also used two different equivalent material models. The first of the equivalent material models uses a localised equivalent material to represent the fractures. This model applies transversely isotropic properties to the finite difference grid points that the fracture occupies in the discrete model. The second equivalent material model uses a homogenous equivalent transversely isotropic material applied to the entire model. The effect of the fractures are averaged over the entire model, to give an equivalent material throughout. The effect of fracture orientation is ignored as the model used in this study is 1D.

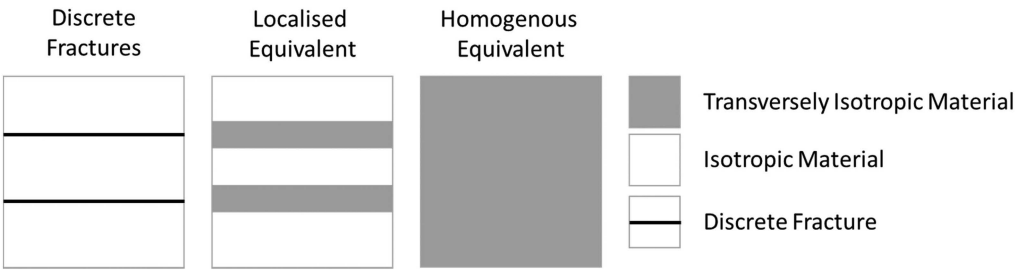

Figure 4. Material models used in analysis.

The appropriate material properties for the different equivalent methods shown in Figure 4 are calculated using crack density (ϵ), which is incorporated into the stiffness matrix for the material (Parastatidis, 2019). Crack density is calculated as the volume of the equivalent material divided by the surface area of each fracture. The calculation of crack density is shown in equation 4, where A and B are the dimensions of the fracture surface, C is the length of the equivalent material and N is the number of fractures. For the homogenous equivalent medium, C is the length of the model, with N being the number of fractures in the entire model; while in the localised medium, C is the length of a single mesh element with N equal to one.

$$\in = \frac{ABC}{ABN} \tag{4}$$

The fractures and the plane of isotropy of the equivalent materials are orientated perpendicular to the direction of propagation of the wave which the model is excited by, as shown by Figure 2. Therefore, the waves will always propagate through the elements which represent the fractures. This allows these materials to modify the wave as it is transmitted. Velocity-time series are recorded in the same place in each model, which are located before and after the fractures. The time series are analysed using a transfer function, displayed in terms of transmission coefficients (TC). TC is calculated using equation 5. This is achieved by taking the Fourier transform of the input wave, before the fractures, and output wave, after the fractures and comparing the amplitude of the frequency components of these. If the amplitude reduces, then the transmission coefficient will be less than 1 and if it increases then it will be greater than one. A reduction in amplitude shows that not all the energy from the incident wave is transmitted through the fractures.

$$TC = \frac{input}{output} \tag{5}$$

3 RESULTS

The model presented in Figure 2, with two fractures, modelled with the different equivalent materials presented in Figure 4, has been solved using the FDM and the results analysed using a transfer function. The results from this are shown in Figure 5. It is clear that there is a similar profile to the transfer functions given by the discrete and localised mediums, with similar frequencies of localised maxima. In the discrete medium these occur at 96 Hz and 843 Hz, while in the localised medium these occur at 92 Hz and 848 Hz. These occur at very similar frequencies to the analytical prediction of the spring resonance, occurring at 96Hz, and the superposition resonance, occurring at 832 Hz, from equations 1 to 3. This shows that the spring and superposition resonance mechanisms occurring in the discrete fractured model also occur in the localised medium, which has not previously been identified. Furthermore, the

similarity in the frequency of the resonances show that the methodology of defining the equivalent medium properties using crack density in equation 4, gives an interface with a near identical stiffness to the discrete fractured model.

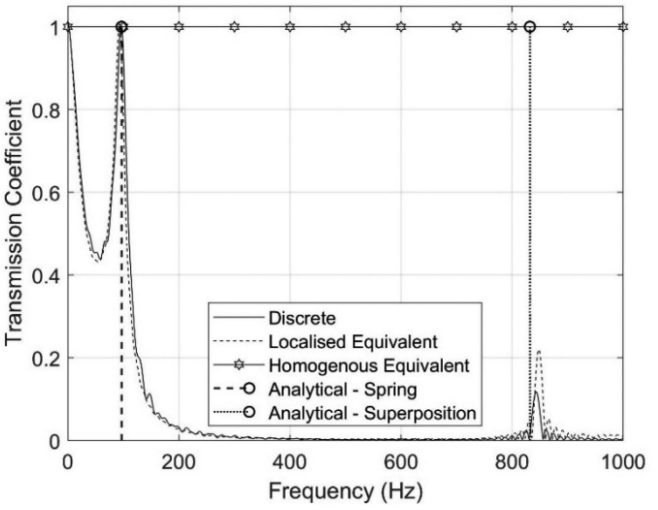

Figure 5. Transfer functions of different representations of a model with two fractures.

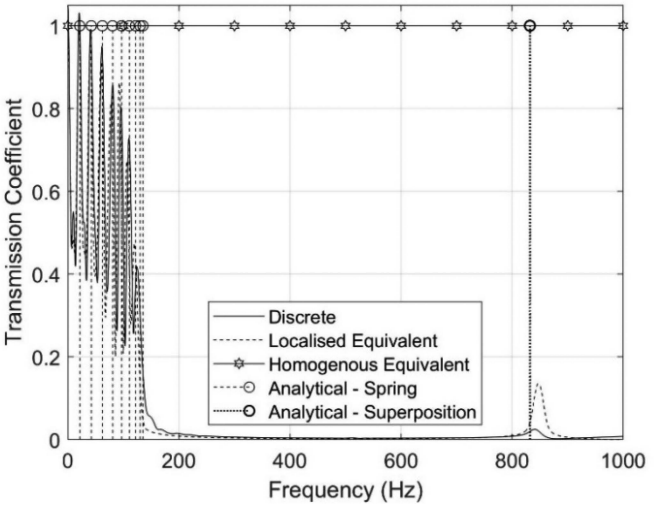

Figure 6. Transfer functions of different representations of a model with ten fractures.

No resonance effects are visible in the homogenous equivalent medium, with the transfer function having a transmission coefficient equal to one at all frequencies. This is the expected result when an elastic wave is transmitted through a continuum without damping applied, such as that in the model outlined in Figure 2. This will still occur despite the transversely isotropic material properties being applied.

Figure 6 shows an extension of the model presented in Figure 2, with ten fractures at a spacing of 2 m, all with identical stiffnesses. The discrete and localised equivalent mediums show similar transfer functions, with localised maxima, representing the resonant frequencies,

occurring at similar frequencies to one another. The analytical resonances are included in this figure, which are shown to be at similar frequencies as the numerical data. The homogenous equivalent medium still shows a transmission coefficient of one at all frequencies. This is despite the increased number of fractures in the model and as such different material properties, as shown by equation 4, giving a different crack density. Therefore, Figure 6 shows that the resonance mechanisms are as relevant in a more complex model with ten fractures, as they did in the simplistic model with two fractures.

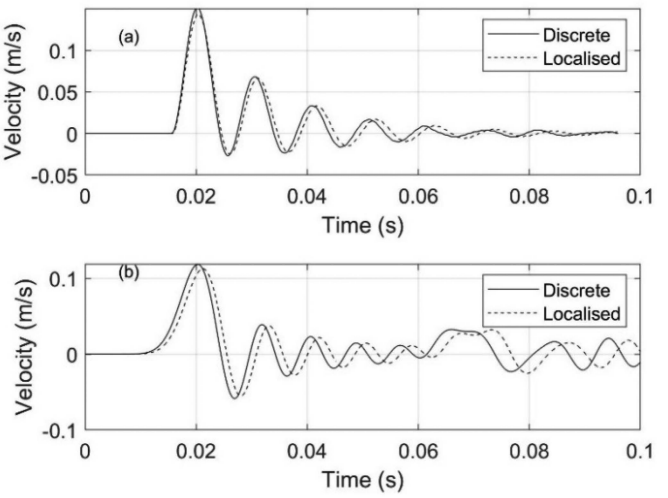

Figure 7. Time series of discrete and localised equivalent models for (a) two fractures and (b) ten fractures.

The velocity-time series recorded after the fractures for the two and ten fractured models are shown in Figure 7. Only results for the discrete and localised material models are shown, as the homogenous equivalent material model does not alter the wave as it passes through. The time series from the homogenous equivalent material model will be identical to the input wave, shown in Figure 3a. In Figure 7 it is possible to identify the two resonant frequencies which can be seen in Figure 5. Both the discrete and localised equivalent mediums show a clear long period oscillation, which appears to dampen as the time series progresses. This is caused by the spring resonance mechanism. This dampening is not a real effect in the model and is in fact caused by the passage of the finite-time wave pulse which is input to the model (Figure 3a). This dampening effect is not so evident in Figure 7b, as the larger number of fractures will cause the wave to move slower through the model, and so spread the wave front out and cause the reduction in amplitude to occur at a later time. In Figure 7a, as the amplitude of the long period oscillation reduces, a shorter period oscillation can be identified in the data. This short period oscillation is caused by the superposition resonance mechanism. This, again, is not so evident in Figure 7b. This is because there are a lot more resonance effects occurring throughout the time series. The nine spring resonance peaks, are themselves very hard to identify in the data, with superposition of these effects occurring to mask each individual resonant frequency. In Figure 7a, the low period oscillation in the localised equivalent material model appears more pronounced than that in the discrete fractured model, which is evidenced by the greater amplitude of the higher frequency resonant peak in the localised equivalent material in Figure 7. There appears to be a slight difference in period between the discrete and localised material models for both the two and ten fractured models. The localised material model seems to have a longer period in both examples shown in Figure 7. This is evidenced in Figure 5, with the localised material having a spring resonance of 92Hz and the discrete

fractured model with a spring resonance of 96Hz. Such effects are likely to occur due to rounding errors associated with the crack density calculation in equation 4.

4 DISCUSSION

Numerical models have been solved in the FDM to identify whether fractured rock mass resonance mechanisms can be identified in equivalent material models. Figures 5 and 6 show that the spring and superposition resonance effects are undoubtedly operating within the discrete fractured and the localised equivalent material models. This is shown by the agreement between the transfer functions of these models and the analytical prediction of the resonance. There are minor differences identified, such as in the slight difference in the spring resonant frequency in Figure 5, although this is likely to be due to rounding errors associated with the calculation of the crack density parameter using equation 4. On the other hand, the same cannot be said for the equivalent medium, which does not alter the wave form as it is transmitted, shown by the transfer function with a transmission coefficient equal to one at all frequencies in Figures 5 and 6. In a non-1D model this would not be the case, as the wave would spread out at different speeds in different directions; therefore, causing the waveform to alter. Despite this, the lack of agreement in this simple 1D scenario, suggests that using an equivalent material for a higher dimensional scenario would not accurately simulate the problem either.

There is a model size related effect in the homogenous equivalent material model in its current form, as used by Parastatidis (2019). Parastatidis (2019) used a small model, entirely populated by fractures, while the model used here is large with fractures only modelled in a small area. This was a necessary step in the models used in this study as they act to remove the effect of reflections form the model boundary. As the crack density calculation, shown by equation 5, uses the volume of the full model, a smaller model with the same number of cracks would have a different crack density. This could give very different material properties purely from a change in the boundary positions. Clearly the homogenous equivalent medium is not appropriate in its current form, requiring modification. However, even if the equivalent medium were applied over a more finite range, such as that which the fractures occupy, then resonance mechanisms are unlikely to develop. This is because the block would not act like a series of masses between springs, especially when the number of fractures is greater than two. Equally, the material velocity in this block would be lower than the material velocity within a block in the discrete model. This will cause the superposition resonance to occur at a different frequency, given by equation 3. Therefore, the use of a more localized homogenous medium will cause the superposition resonance to be altered. This will occur regardless of whether there are two fractures or multiple fractures.

The implications of this work is that, even when the wavelength of the transmitted wave is much longer than the fracture spacing, homogenous equivalent materials will not accurately represent the seismic response of a fractured medium. Therefore, for application to train vibrations in fractured rock masses, it is necessary to use a model that simulates fractures either discretely or by using a localized equivalent medium, in order to give accurate predictions of vibrations. A more accurate prediction will give a better indication of the likely magnitude of vibrations at a receiver allowing appropriate mitigation measures to be implemented.

5 CONCLUSION

Vibrations from railway lines are common in the modern built environment and can have consequences for the use of buildings and the health of residents. Mitigation of such vibrations reduces their impact. Accurate prediction of the vibrations incident upon a receiver allows appropriate mitigation measures to be designed. This study has analysed the fractured rock mass resonance effects of spring and superposition resonance using equivalent material

models. This was achieved using a numerical model solved using the finite difference method. Fractures have been modelled discretely, using special elements within the finite difference mesh, as well as by using localized equivalent materials and homogenous equivalent materials. Transfer functions have been derived which show how the amplitude of different frequencies of waves transmitted through the model change. The homogenous equivalent material is shown to have a transmission coefficient equal to one at all frequencies; therefore, removing all resonance effects from the fractured rock mass. However, the discrete and localised equivalent materials show resonances within the transfer functions that closely match the predicted frequencies from the analytical equations for the spring and superposition resonance effects. There are minor differences between the frequencies of the resonances in these cases, although these are identified as being caused by rounding errors in the crack density calculation, which is used to generate the material properties for the equivalent materials. Therefore, a localised equivalent material model has been shown to match closely with the response of a discrete fracture model, which gives scope to use more diverse models to predict such vibrations.

REFERENCES

Avci O, Bhargava A, Nikitas N, Inman DJ. Vibration annoyance assessment of train induced excitations from tunnels embedded in rock. Sci Total Environ 2020;711:134528.

Bandis SC, Lumsden AC, Barton NR. Fundamentals of rock joint deformation. Int. J. Rock Mech. Min. Sci. Geomech. Abstr., vol. 20, 1983, p. 249–68.

Cai JG, Zhao J. Effects of multiple parallel fractures on apparent attenuation of stress waves in rock masses. Int J Rock Mech Min Sci 2000;37:661–82.

Deng XF, Zhu JB, Chen SG, Zhao J. Some fundamental issues and verification of 3DEC in modeling wave propagation in jointed rock masses. Rock Mech Rock Eng 2012;45:943–51.

Eitzenberger A. Wave propagation in rock and the influence of discontinuities. Luleåtekniska universitet, 2012.

Fan LF, Wang LJ, Wu ZJ. Wave transmission across linearly jointed complex rock masses. Int J Rock Mech Min Sci 2018;112:193–200.

Forrest JA, Hunt HEM. Ground vibration generated by trains in underground tunnels. J Sound Vib 2006;294:706–36.

Hildyard MW. Manuel Rocha Medal Recipient Wave interaction with underground openings in fractured rock. Rock Mech Rock Eng 2007;40:531–61.

Hildyard MW, Daehnke A, Cundall PA, others. WAVE: A computer program for investigating elastodynamic issues in mining. 35th US Symp. rock Mech., 1995.

Holmes H, Paraskevopoulou C, Hildyard MW, Connolly DP, Neaupane K. Numerical Modelling of Resonance Mechanisms in Jointed Rocks using Transfer Functions. J Rock Mech Geotech Eng 2022;15. https://doi.org/https://doi.org/10.1016/j.jrmge.2022.09.001.

Hussein MFM, François S, Schevenels M, Hunt HEM, Talbot JP, Degrande G. The fictitious force method for efficient calculation of vibration from a tunnel embedded in a multi-layered half-space. J Sound Vib 2014;333:6996–7018.

Hussein MI, Leamy MJ, Ruzzene M. Dynamics of phononic materials and structures: Historical origins, recent progress, and future outlook. Appl Mech Rev 2014;66.

Li S, Tian S, Li W, Yan T, Bi F. Research on the resonance characteristics of rock under harmonic excitation. Shock Vib 2019;2019.

Nakagawa S. Acoustic resonance characteristics of rock and concrete containing fractures. University of California, Berkeley; 1998.

Parastatidis E. How do seismic waves respond to fractures in rock? Evaluation of effective media versus discrete fracture representations. University of Leeds, 2019.

Pyrak-Nolte LJ, Myer LR, Cook NGW. Transmission of seismic waves across single natural fractures. J Geophys Res Solid Earth 1990;95:8617–38.

Ruiz JF, Soares PJ, Costa PA, Connolly DP. The effect of tunnel construction on future underground railway vibrations. Soil Dyn Earthq Eng 2019;125:105756.

Sheng X. A review on modelling ground vibrations generated by underground trains. Int J Rail Transp 2019;7:241–61.

Xu C, Liu Q, Wu J, Deng P, Liu P, Zhang H. Numerical study on P-wave propagation across the jointed rock masses by the combined finite-discrete element method. Comput Geotech 2022;142:104554.